Non-dissipative energy capture of confined liquid in nanopores

Baoxing Xu,[1] Xi Chen,[1] Weiyi Lu,[2] Cang Zhao,[2] and Yu Qiao[2,3,a)]
[1]*Columbia Nanomechanics Research Center, Department of Earth & Environmental Engineering, Columbia University, New York, New York 10027, USA*
[2]*Department of Structural Engineering, University of California–San Diego, La Jolla, California 92093-0085, USA*
[3]*Program of Materials Science and Engineering, University of California–San Diego, La Jolla, CA 92093, USA*

(Received 6 January 2014; accepted 3 May 2014; published online 21 May 2014)

In the past, energy absorption of protection/damping materials is mainly based on energy dissipation, which causes a fundamental conflict between the requirements of safety/comfort and efficiency. In the current study, a nanofluidic "energy capture" system is reported, which is based on nanoporous materials and nonwetting liquid. Both molecular dynamics simulations and experiments show that as the liquid overcomes the capillary effect and infiltrates into the nanopores, the mechanical energy of a stress wave could be temporarily stored by the confined liquid phase and isolated from the wave energy transmission path. Such a system can work under a relatively low pressure for mitigating high-pressure stress waves, not necessarily involved in any energy dissipation processes. © *2014 AIP Publishing LLC*. [http://dx.doi.org/10.1063/1.4878097]

When a projectile impacts another solid surface, severe damages may be caused on both sides as high-pressure stress waves are generated. To protect personnel and important infrastructures and devices, protection or damping materials are often employed to "absorb" the mechanical energy. Such an energy absorption process is essential in almost every aspect of human activities,[1,2] and the important factors that govern the generation, propagation, transmission, and reflection of intense stress waves have been an active area of research for decades.[3–6] Inspired by these studies, a large number of energy absorption materials (EAMs) were developed, such as composite materials,[7–9] granular materials,[10,11] and foams and honeycombs.[12–15] The working mechanisms of these conventional EAMs are mostly based on energy dissipation—conversion of mechanical energy to thermal energy. For instance, as a foam is subjected to a sufficiently high load (P), the cell walls would buckle, which dissipates a considerable portion of mechanical work.[16] The energy absorption capacity can be assessed as $E = P_w \cdot V_r$, where P_w is the pressure at which the energy absorption process, e.g., cell wall buckling in the example of a foam, is activated and V_r is the associated volume reduction. Study has been conducted on energy trapping concepts,[17] while the results are still not fully conclusive.

For a dissipative EAM, on the one hand, to reach a high energy absorption capacity (E), the energy absorption pressure (P_w) must be as high as possible—but lower than the applied load (P); otherwise, the EAM would behave as a rigid body and no energy absorption can take place. On the other hand, the pressure of the transmitted stress wave that reaches the target to be protected, P_t, can only be equal to or higher than the energy absorption pressure (P_w), since below P_w no energy absorption mechanism can be activated; therefore, for safety and comfort, P_w should be as low as possible. While using functionally graded materials may help accommodate the conflict between these two opposite requirements, when the required P_t is low and the impact/blast load (P) is high, there is still no satisfactory solution. For example, to develop a blast mitigation helmet, the high blast pressure, often on the scale of 10^2 psi,[18] must be reduced to a few psi by using a thin, lightweight protection pad so as to avoid traumatic brain injury (TBI),[19,20] which is still a blank area of today's technology.

In order to circumvent the intrinsic problem of conventional EAMs discussed above, at least one more degree of freedom must be introduced into the protection system, for which "energy capture" (EC),[21] a non-dissipative energy absorption mechanism that will be discussed in detail below, provides a promising approach.

During wave propagation, if the energy-carrying medium can be interrupted by a container, and, more importantly, if the wave energy cannot immediately transmit through the container, the wave energy is effectively "captured." Different from an energy dissipation process, the captured wave energy is not necessarily converted to other forms of energy, e.g., heat, but simply stored temporarily and isolated from the original energy transmission path. Thus, the pressure of the transmitted wave that would reach the target (P_t) can be much lowered.

To achieve a high EC efficiency, not only the energy-carrying medium needs to be confined, but also the energy that can go through the walls of the confinement should be minimized. In an ideal case where no wave energy transmission across the confinement wall can occur, the EC capacity can be estimated as $E = P \cdot V_r$, not $P_{in} \cdot V_r$, where P_{in} is the critical pressure at which the EC mechanism works—the counterpart of P_w of a conventional EAM. That is, the EC capacity is independent of P_{in}: The protection/damping system can work at a low pressure (P_{in}) and "capture" the energy carried by a high-pressure (P) wave, and, therefore, be safe/comfortable and also energetically efficient at the same time.

One possible method to realize energy capture is to use a nanoporous material, immersed in a non-wetting liquid (Figure 1). The nanopores are initially empty. As a high-pressure (P) stress wave propagates in the liquid medium, if

a)Author to whom correspondence should be addressed. Electronic mail: yqiao@ucsd.edu. Tel.: +1-858-534-3388. Fax: +1-858-534-1310

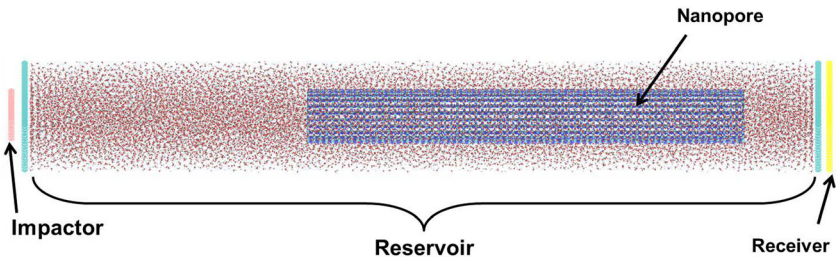

FIG. 1. The MD computational cell for simulating an EC system consisting of a nanoporous material and a non-wetting liquid. The system is formed by an impactor, a piston, a water reservoir, a silica nanopore, boundary planes of reservoir, and a receiver (from left to right). The impactor is rigid to mimic a foreign impact loading parallel with the axial direction of the nanopore with a velocity of v; the piston, i.e., the left boundary plane of reservoir, is movable and modeled by a rigid plane; the nanopore is immersed into the reservoir; the right rigid boundary plane of reservoir is also movable. The receiver is fixed throughout the MD simulation and is used to deduce the transmitted force through the nanopore/water system. A periodical boundary condition is imposed to the four lateral planes of the cell. Upon the pressure of a stress wave on this system, the water molecules become highly compressed and can infiltrate into the nanopore. The invaded molecules rearrange themselves in a relatively ordered configuration. Within a short time frame, a large amount of wave energy can be transferred into the potential energy of the confined water molecules, which does not transmit across the nanopore walls, leading to a substantial stress-wave mitigation effect.

P is higher than the critical infiltration pressure (P_{in}), the liquid phase can overcome the capillary resistance and rapidly infiltrate into the nanopores. The duration of liquid infiltration ranges from nanoseconds (ns) to microseconds (μs), as the system parameters, such as nanopore size, nanopore depth, and wave energy, vary. The confined liquid phase is highly compressed and carries the wave energy, on the order of $P \cdot V_{\text{r}}$, which may not transmit out through the relatively incompressible nanopore walls and is effectively "captured," in the form of potential energy among the confined liquid molecules. Upon unloading, the confined liquid may or may not defiltrate out of the nanopores, depending on the nanopore configuration and the inner surface properties. Even if the liquid defiltrates out, it tends to happen at a much slower rate compared with the infiltration process, so that the captured energy is released only gradually.

In such a process, the system volume reduction, V_{r}, is close to the porosity, typically 30–90%. The higher the wave pressure, P, is (i.e., the more intense stress wave is), the larger the stress wave mitigation capacity would be. The EC activation pressure (P_{in}) is determined by the effective interface tension of the confined liquid at nanopore walls, unrelated to the wave pressure.

To validate this concept, both MD simulations and experiments were carried out. Figure 1 illustrates the computational model, where a segment of hydrophobic (16,16) silica nanotube (SNT) with the length of 19.6 nm and the diameter of 2.17 nm is immersed in a water reservoir, whose size is $3.6 \times 3.6 \times 35.5$ nm^3, containing 14772 water molecules. The SNT is aligned with the impact direction. The reservoir is bounded by two rigid carbon planes and is deformable, and its left end is impacted by an impactor. The impactor, a rigid mass, collides the reservoir with a given initial velocity (v), generating a pressure wave traveling from the left to the right. The whole system would move toward the right, and will hit a receiver, a rigid carbon plane fixed in space. Afterwards, the system will bounce back and the impactor may detach from the reservoir. The history of the stress wave transmitted to the receiver is recorded. A periodical boundary condition is imposed on the four lateral planes of the computational cell. For comparison, a reference system is setup with an almost identical structure, except that the SNT is end-capped so that water infiltration cannot occur. The 12–6 Lennard-Jones (L-J) empirical force field and a Coulomb potential is used to describe the intermolecular potential between atoms. The particle-particle and particle-mesh (PPPM) technique with a root mean square accuracy of 10^{-4} is employed to handle the long range Coulomb interactions among water molecules. The L-J interactions are truncated at a cutoff distance of 10 Å. The water model is an extended simple point charge model (SPC/E). After initial equilibrium calculation to minimize system energy, the NVE ensemble is employed to monitor the transmitted force and the number of confined water molecules inside the nanopore. The simulation is performed using the molecular dynamics program LAMMPS. More details of the MD simulation are given in the supplementary material.[22]

Upon the impact, the system (the reservoir containing the SNT) moves toward the receiver (See the snap shots from MD simulations at the impact velocity of 50 m/s in Figure S1),[22] as the liquid pressure (P) builds up. The highly compressed water molecules invade the SNT, since $P > P_{\text{in}}$, converting a part of the incoming wave energy to the potential energy of infiltrated water molecules, and weakening the magnitude and the rate of the transmitted stress wave. After the impactor bounces back, the pressure inside the water reservoir is reduced, and the confined water molecules recede. Figure 2(a) gives the history of transmitted force, which increases with infiltration, and it peaks at almost the same time when the SNT is filled by the compressed water molecules. It then decreases at a slower rate upon unloading. Comparing with the reference system, the peak load arrives later, and the force reduction is prominent. Define the reduction of the peak transmitted force as $\Delta F = (|F_{\max} - F'_{\max}|)/F'_{\max}$, where $F_{\max}$ and $F'_{\max}$ are the maximum transmitted forces in the EC system and the reference system, respectively. For the present system, $\Delta F = 53\%$. The energy of transmitted impulse can be estimated as $E = \xi \int_0^t F^2 dt$, with ξ being a system parameter, and its reduction (ΔW) is around 57%. When the impact velocity decreases to 30 m/s (Figure 2(b)), $\Delta F = 44\%$ and $\Delta W = 64\%$.

To estimate the captured energy, we calculate the ratio between the variation of potential energy of the infiltrated molecules (at the instant of the peak transmitted force and with respect to that of bulk ambient water) and the incoming wave energy, $E_{capture}/E_{input}$. Figure 3 shows that $E_{capture}/E_{input}$ increases with v when v is relatively low, and

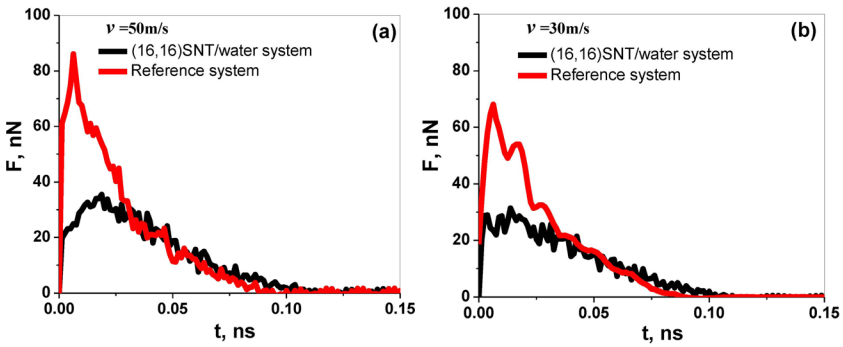

FIG. 2. The history of the transmitted force under impact velocities of (a) $v = 50$ m/s and (b) $v = 30$ m/s, respectively.

it reaches a maximum value, as much as 40% for the present SNT geometry, at about 50 m/s. The ratio of $E_{capture}/E_{input}$ then gradually reduces as v further increases. When the impact velocity is slow, the infiltration process is less prominent and the SNT may not be filled, and, thus, the EC efficiency tends to be low. With the increase of v, more water molecules infiltrate into the nanopore, and their associated potential energy is captured. Moreover, the reordering of confined water molecules in nanopores may increase the EC capacity. The maximum potential energy of water molecules that may be captured by the nanopore depends on both pore geometry and impact velocity. If v is higher than 50 m/s, although the confined water molecules can be more compacted and the absolute value of $E_{capture}$ is high, the increase in incoming wave energy is more pronounced; hence, $E_{capture}/E_{input}$ is lowered. Due to the weak hydrophobicity and the smoothness of the SNT inner surface, the contribution of the captured energy is much more prominent than the excessive interfacial energy and frictional effects.[23,24]

The above MD simulation was inspired and guided by an earlier split Hopkinson bar (SHB) experiment on a hydrophobic nanoporous silica gel, with the average nanopore size of about 100 nm. In a stainless steel cylinder, a certain amount of hydrophobic silica gel was immersed in a saturated lithium chloride (LiCl) solution. The silica to liquid mass ratio ranged from 0% to 8.2%, and the sample thickness was maintained as 10 mm. The cylinder was sealed by two stainless steel pistons at both ends. A striker was projected onto the incident bar connected to the front piston, and through the impact an incident stress wave was generated. The pressure wave was partly reflected at the interface of the piston and the liquid phase, and the transmitted pulse was measured by a strain gage on the transmitted bar firmly connected to the back piston. More details of the material preparation, the testing setup, and the data analyses are discussed in the supplementary material.[22] Note that the striker is not the counterpart of the impactor in the computer simulation. The computer-simulated structure can be regarded as a local area of liquid surrounding a single nanopore, and the impactor is merely a numerical approach to set the initial condition of stress wave.

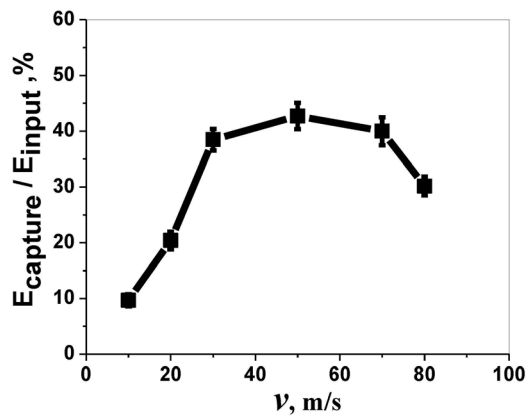

FIG. 3. The ratio between the captured potential energy of water molecules inside SNT and the total input wave energy.

Figure 4 shows the typical measurement results. The impact rate was 5 m/s, and the effective strain rate was around 3×10^2/s. The incident stress waves in all the tests were nearly the same. A reference curve was measured by using a similar experimental setup containing only neat liquid; i.e., no silica gel was added. Due to the impedance mismatch between the steel and the liquid phase, a part of the incident wave would be reflected and, even little energy dissipation took place, only a portion of the wave could transmit through the testing cell. Additional reference tests were conducted on hydrophilic silica particles, obtained by heating the hydrophobic silica gel at 450 °C for 2 h, so that the organic coating was removed;[25] everything else remained the same. The amount of hydrophilic silica was 0.1 g.

Figure 4(a) indicates that, when the amount of hydrophobic silica gel (m) is relatively small, the transmitted wave is close to that of the reference neat-liquid sample. As m increases, the transmitted wave pressure is considerably reduced. When the hydrophobic silica amount is 0.1 g, the transmitted wave almost vanishes, i.e., most of the wave energy is absorbed. In comparison, the control sample containing 0.1 g of hydrophilic silica has a similar system configuration, except that the silica particles are spontaneously soaked up and, therefore, no liquid infiltration would occur during the SHB test. As shown by Fig. 4(b), the transmitted wave pressure of the hydrophilic-silica control sample is even higher than that of the neat-liquid sample, suggesting that the variation in wave pressure is dominated by liquid motion in nanopores. The difference between the hydrophilic-silica sample and the neat-liquid sample may be related to the shear thickening effect of the silica particles.[26]

Under the dynamic loading, the captured specific energy can be assessed as $E_C = E_0 - E_T \sim 20$ J/g, where $E_0 = E_I - E_R$ is the effective input wave energy to the testing sample, E_I is the incident wave energy, E_R is the reflected wave energy, and E_T is the transmitted wave energy. The value of E_C is much higher than the nominal energy dissipation capacity of the hydrophobic silica gel, around 2.5 J/g, measured under a

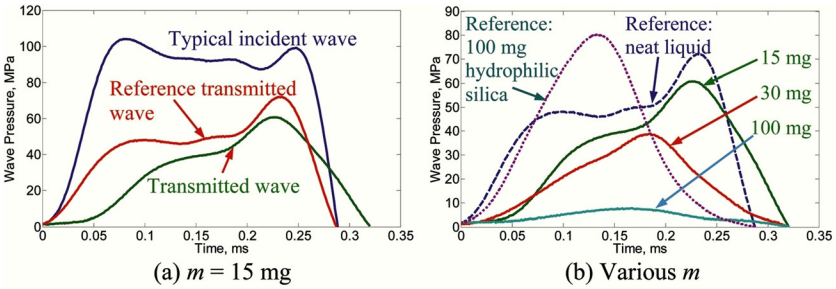

FIG. 4. The energy capture effect of a nanoporous silica gel immersed in a nonwetting liquid: (a) The incident and the transmitted waves of a sample containing 15 mg of hydrophobic silica gel; the reference curve is the transmitted wave of neat liquid. (b) The transmitted waves of samples of different amounts of hydrophobic silica gel.

quasi-static loading condition (see supplementary material[22]), fitting well with the MD prediction and suggesting that non-dissipative energy capture may be the major wave energy absorption mechanism. Under the dynamic testing condition, the pressure of the stress wave by far exceeds the infiltration pressure of the nanopores, and the micro/nano-structure of the silica-liquid system changes significantly as the wave advances across it. The wave behaviors cannot be analyzed by linear wave theory, and the large variation in transmitted wave energy may not be fully explained by the reduction in effective density of the liquid phase. For instance, it has been demonstrated experimentally that the effect of air bubbles in liquid samples on the transmission of intense stress waves is only secondary.[27] Note that the comparison between the MD simulation and the experiment is qualitative, due to the limitation of the size and time scales accessible to MD simulations.

In summary, through molecular simulations and experiments on a nanoporous silica based system, we have demonstrated a promising, non-dissipative energy absorption mechanism—energy capture, for mitigation of intense stress waves of impact, collision, and blast. Upon a dynamic loading, a significant part of the stress wave energy can be converted to the potential energy of infiltrated liquid phase in nanopores. The captured energy is temporarily confined, which greatly reduces the pressure and the energy of the transmitted stress wave. The effects of key system parameters are under investigation. In the materials under investigation, the captured energy is later gradually released after the impact process ends.

The concept generation, the theoretical analysis, and the system design were supported by the National Science Foundation under Grant No. ECCS-1028010. The experimental investigation was supported by the Army Research Office under Grant No. W91CRB-11-C-0112, and the materials preparation was supported by DARPA under Grant No. W91CRB-11-C-0112 (subaward to UCSD). The program development for the computer simulation was supported by the National Science Foundation under Grant No. CMMI-0643726. The computational case study was supported by DARPA under Grant No. W91CRB-11-C-0112 (subaward to Columbia University). The data analysis of computer simulation was supported by the Natural Science Foundation of China under Grant No. 11172231.

[1]G. Lu and T. Yu, *Energy Absorption of Structures and Materials* (CRC Press, Hong Kong, 2003).
[2]J. McKittrick, P. Chen, L. Tombolato, E. E. Novitskay, M. W. Trim, G. A. Hirata, E. A. Olevsky, M. F. Horstemeyer, and M. A. Meyers, Mater. Sci. Eng. C **30**, 331–342 (2010).
[3]S. W. Cranford, A. Tarakanova, N. M. Pugno, and M. J. Buehler, Nature **482**, 72–78 (2012).
[4]H. Gao, B. Ji, I. L. Jäger, E. Arzt, and P. Fratzl, Proc. Natl. Acad. Sci. U.S.A. **100**, 5597–5600 (2003).
[5]J. Aizenberg, J. C. Weaver, M. S. Thanawala, V. C. Sundar, D. E. Morse, and P. Fratzl, Science **309**, 275–278 (2005).
[6]K. Tai, M. Dao, S. Suresh, A. Palazoglu, and C. Ortiz, Nature Mater. **6**, 454–462 (2007).
[7]L. F. Wang, J. Lau, E. L. Thomas, and M. C. Boyce, Adv. Mater. **23**, 1524–1529 (2011).
[8]B. N. Cox, N. Sridhar, J. B. Davis, X.-Y. Gong, and F. W. Zok, Acta Mater. **48**, 755–766 (2000).
[9]D. D. Dubey and A. J. Vizzini, J. Compos. Mater. **32**, 158–176 (1998).
[10]R. Carretero-González, D. Khatri, M. A. Porter, P. G. Kevrekidis, and C. Daraio, Phys. Rev. Lett. **102**, 024102 (2009).
[11]V. F. Nesterenko, "Shock (Blast) Mitigation by "Soft" Condensed Matter" in *Granular Material-Based Technologies*, MRS Symp. Proc., Vol. 729 (MRS, Pittsburgh, PA, 2003), pp. MM4.3.1–4.3.12.
[12]T. A. Schaedler, A. J. Jacobsen, A. Torrents, A. E. Sorensen, J. Lian, J. R. Greer, L. Valdevit, and W. B. Carter, Science **334**, 962–965 (2011).
[13]A. G. Evans, J. W. Hutchinson, N. A. Fleck, M. F. Ashby, and H. N. G. Wadley, Prog. Mater. Sci. **46**, 309–327 (2001).
[14]A. H. Brothers and D. C. Dunand, Scr. Mater. **54**, 513–520 (2006).
[15]A. Cao, P. L. Dickrell, W. G. Sawyer, M. N. Ghasemi-Nejhad, and P. M. Ajayan, Science **310**, 1307–1310 (2005).
[16]L. J. Gibson and M. F. Ashby, *Cellular Solids: Structure and Properties* (Cambridge University Press, Cambridge, 1997).
[17]J. Hong, Phys. Rev. Lett. **94**, 108001 (2005).
[18]C. E. Needham, *Blast Waves (Shock Wave and High Pressure Phenomena)* (Springer, 2010).
[19]A. Courtney and M. Courtney, Med. Hypotheses **72**, 76–83 (2009).
[20]M. Nyein, A. M. Jason, L. Yu, C. M. Pita, J. D. Joannopoulos, D. Moore, and R. Radovitzky, Proc. Natl. Acad. Sci. U.S.A. **107**, 20703–20708 (2010).
[21]W. Lu, B. J. Chow, T. Kim, A. Han, and Y. Qiao, Appl. Phys. Lett. **98**, 013102 (2011).
[22]See supplementary material at http://dx.doi.org/10.1063/1.4878097 for the details of computer simulation and experimental procedure.
[23]X. Chen, G. Cao, A. Han, V. K. Punyamurtula, L. Liu, P. J. Culligan, T. Kim, and Y. Qiao, Nano Lett. **8**, 2988 (2008).
[24]K. Falk, F. Sedlmeier, L. Joly, R. R. Netz, and L. Bocquet, Nano Lett. **10**, 4067 (2010).
[25]A. Han, V. K. Punyamurtula, and Y. Qiao, Chem. Eng. J. **139**, 426 (2008).
[26]M. J. Decker, C. J. Halbach, C. H. Nam, N. J. Wagner, and E. D. Wetzel, Compos. Sci. Technol. **67**, 565 (2007).
[27]K. Ando, T. Sanada, K. Inaba, J. S. Damazo, J. E. Shepherd, T. Colonius, and C. E. Brennen, J. Fluid Mech. **671**, 339 (2011).